

# Sensitivity of the subpolar North Atlantic to Last Glacial Maximum surface forcing and sea ice distribution in an eddy-permitting regional ocean model

Duo Yang,<sup>1</sup> Paul G. Myers,<sup>1</sup> and Andrew B. G. Bush<sup>1</sup>

Received 27 August 2005; revised 2 February 2006; accepted 14 February 2006; published 18 May 2006.

[1] The impact of paleoatmospheric forcing and sea ice distribution on the circulation of the subpolar North Atlantic is examined in a regional eddy-permitting ocean model. We focus on water mass formation and the pathway of the North Atlantic Current. Paleofluxes are obtained from a coupled atmospheric general circulation model, while the seasonal sea ice cover is based on a pair of Last Glacial Maximum sea ice reconstructions. Labrador Sea Water formation, the pathway of the North Atlantic Current, and the strength of the Atlantic Meridional Overturning Circulation are found to be dependent on the structure of the sea ice representation. Here, the key role played by the sea ice is its isolation of the underlying ocean from the wintertime atmospheric fluxes. The results highlight the need for accurate seasonal sea ice fields for validating paleomodeling simulations.

**Citation:** Yang, D., P. G. Myers, and A. B. G. Bush (2006), Sensitivity of the subpolar North Atlantic to Last Glacial Maximum surface forcing and sea ice distribution in an eddy-permitting regional ocean model, *Paleoceanography*, 21, PA2013, doi:10.1029/2005PA001209.

## 1. Introduction

[2] The importance of the subpolar North Atlantic in climate change is connected to its role in poleward heat transport. This is linked to Labrador Sea deep convection and hence the formation of Labrador Sea Water (LSW), as well as the North Atlantic Current (NAC), an extension of the Gulf Stream [Clarke *et al.*, 1980]. Currently, the former, one component of the North Atlantic Deep Water (NADW), helps to drive the sinking branch of the meridional overturning circulation (MOC), a global system of surface and subsurface ocean currents, while the latter is unique as an upper layer branch in transporting warm waters to much higher latitudes than in any other ocean [Rossby, 1996]. Both of them have displayed interannual and interdecadal variability over the last five decades [Dickson *et al.*, 1996; Curry *et al.*, 1998; Curry and McCartney, 2001]. LSW formation and the NAC experienced major fluctuations between today and the last glacial period. The Last Glacial Maximum (LGM, about 22 to 14 kyr B.P.) was characterized by significantly lower temperature than today with large continental areas covered by great ice sheets and a consequent sea level drop of 121 m [Fairbanks, 1989] with extensive sea ice in the northern latitudes [Crowley and North, 1991].

[3] Paleoproxy data have provided us with some evidence in terms of the discrepancy in water mass formation and

heat transport during the LGM, in comparison with modern values. Weakening and shallowing of NADW [e.g., Curry and Lohmann, 1983; Oppo and Fairbanks, 1987; Boyle and Keigwin, 1987; Veum *et al.*, 1992], with a shift in its formation to relatively southern latitudes [Alley and Clark, 1999], were deduced from the decreased flux of NADW into the Southern Ocean [Oppo and Fairbanks, 1987; Rutberg *et al.*, 2000] and consequently a further northward penetration of South Ocean Water (SOW) into the benthic Atlantic Ocean [Marchitto *et al.*, 2002]. With the southward shift of NADW formation came a similar shift in the Gulf Stream/NAC system which became more zonally orientated [Ruddiman and McIntyre, 1977, 1984; CLIMAP, 1981]. Consequently, poleward ocean heat transport in the North Atlantic was reduced [Miller and Russell, 1989]. Weakening and shallowing of the NADW [e.g., Weaver *et al.*, 1998, 2001; Seidov *et al.*, 1996] with a southward shift [e.g., Seidov and Haupt, 1997], as well as reduced poleward heat transport [e.g., Seidov and Maslin, 1996], have been reproduced in coupled and ocean-only models configured for the LGM. Cottet-Puinel *et al.* [2004] note from their simulations of the last glacial cycle that the MOC systematically weakens when LSW formation ceases and strengthens when it resumes.

[4] The sensitivity of water mass formation and the ocean circulation to changes in North Atlantic surface fluxes has become a major factor in explaining climate variability. From reconstructions, [de Vernal and Hillaire-Marcel, 2000; de Vernal *et al.*, 2002] infer a strong stratification between a low saline surface layer (due to seasonal sea ice spreading) and the underlying waters, implying diminished LSW formation. Keffer *et al.* [1988] and Bush and

<sup>1</sup>Department Earth and Atmospheric Sciences, University of Alberta, Edmonton, Alberta, Canada.

*Philander* [1999] attribute the southward migration in the Gulf/NAC system to the prevailing wind field modified by the great ice sheets [*Manabe and Broccoli*, 1985] 3500–4000 m thick (e.g., the Laurentide in eastern North America) [e.g., *CLIMAP*, 1981].

[5] Sea ice can alter sea surface salinity (hence the density), therefore stratification and vertical convection of the water column, as suggested by [*de Vernal and Hillaire-Marcel*, 2000; *de Vernal et al.*, 2002], as well as limit the energy and mass exchanges at the ocean-atmosphere interface. Our focus here is to investigate the impact of atmospheric and sea ice forcing on the circulation of the subpolar North Atlantic during the LGM. We carry this out by focusing on LSW formation (and thus variations in strength for the Atlantic MOC, AMOC) as well as the pathway of the NAC. We choose the LGM since this is a period during which it is easiest to construct a permanently or seasonally ice covered Labrador Sea. We will show that cold water would be able to speed up the AMOC when the sea surface is ice free, and this process is curtailed by the existence of the sea ice coverage either permanently or seasonally. The tool we use is a high-resolution eddy-permitting ocean model of the subpolar North Atlantic. We feel this tool is consistent with our focus, since coarser resolution (and consequently poorer representation of eddy and frontal processes) can lead to a weakening and broadening of frontal features and currents (including the NAC). Section 2 describes briefly the model configuration and experiment design, as well as the ocean-atmosphere general circulation model (CGCM) output (similar to that of *Bush and Philander* [1999]) and sea ice reconstructions [*Crowley and North*, 1991; *de Vernal and Hillaire-Marcel*, 2000] that we use as forcing. The model results are analyzed in section 3, followed by a discussion and summary in section 4.

## 2. A Brief Description of the Model and Experiment Design

[6] The model is a flux-forced version [*Yang*, 2005] of a regional eddy-permitting ( $1/3^\circ$ ) ocean model of the subpolar North Atlantic ( $\sim 68^\circ\text{W}$ – $0^\circ$ , and  $\sim 38$ – $70^\circ\text{N}$ ) [*Myers*, 2002] having 36 unevenly spaced vertical  $z$  levels. The model also features a finite volume partial cell [*Adero et al.*, 1997] topography, taken from ETOPO5 [*NOAA*, 1988] data set, as well as open boundary conditions dealing with connections with the rest of the Atlantic Ocean at  $38^\circ\text{N}$  and buffer zones used in the northern boundary regions. The model is described in more detail by *Myers* [2002].

[7] For our present-day control run, the climatological surface buoyancy (heat and freshwater) forcing originates from ship/buoy measurements of the Southampton Oceanography Center (SOC) [*Josey et al.*, 1998] (mean of 1980–1993), with the addition of a crude parameterization of the effect of high-frequency variability resulting from the passages of synoptic scale events on the heat flux (fivefold of SOC mean) over the convective region of the Labrador Sea ( $\sim 55$ – $59^\circ\text{N}$  and  $\sim 51$ – $56^\circ\text{W}$ ) during November–March so as to improve the climatological representation of water mass formation and model hydrography. The focus on this region is that the deep convection in the Labrador Sea is

very localized and has mainly been observed in the western interior of the basin, around  $56$ – $58^\circ\text{N}$  and  $52$ – $55^\circ\text{W}$  [*Clarke and Gascard*, 1983; *Wallace and Lazier*, 1988; *Lilly et al.*, 1999]. Wind stress is from the European Center for Medium Range Weather Forecast (ECMWF) climatology, assembled by *Trenberth et al.* [1990] for the period 1980–1986. Note that we do not use the SOC wind stress climatology since it is not complete in the subpolar gyre, as it does not include data in seasonally ice covered regions. For the southern open boundary, the tracers are allowed to be advected or diffused out of the domain if the velocities (perpendicular to the boundary) at some level are directed out of the domain, and are restored smoothly to climatology [*Lozier et al.*, 1995; *Grey and Haines*, 1999] if the velocities are directed into the domain. The northern boundary is closed with restoring buffers in Hudson Strait, Baffin Bay and the region to the north of the Iceland [*Myers*, 2002]. The configuration thus manifests the important processes associated with water mass formation and dispersal, as well as circulation in this region at the present day [see *Yang*, 2005].

[8] Paleofluxes (both buoyancy fluxes and wind stress) are taken from a 70-year CGCM configured for the LGM (21 kyr B.P.), as described by *Bush and Philander* [1999]. Since the direct application of CGCM surface fluxes to force an OGCM can lead to model instability and drift [*Rosati and Miyakoda*, 1988], the paleoheat and freshwater flux forcing used is obtained by adding anomalies derived from two CGCM simulations (LGM minus control) (Figure 1) to the present-day flux fields used in the control experiment. The major features are much stronger heat losses over the Labrador Sea at the LGM, associated with strong northwest prevailing winds off the ice cap [*Manabe and Broccoli*, 1985; *Bush and Philander*, 1999]. These winds also lead to strong evaporation and low precipitation and thus freshwater losses over the Labrador Sea. Together, this forcing implies significantly greater buoyancy loss over the Labrador Sea and hence denser surface waters. In contrast, increased precipitation under the stronger Atlantic storm track decreases surface salinity toward the southern end of our domain.

[9] The CGCM has a limited (thermodynamic) representation of sea ice. In the LGM simulation, the sea ice is confined to a region north of  $61^\circ\text{N}$  to the west of Greenland and north of  $66^\circ\text{N}$  to the east of Greenland (Figure 2). A comparison with two different reconstructions of sea ice [*Crowley and North*, 1991; *de Vernal and Hillaire-Marcel*, 2000] implies an underestimation of sea ice in the CGCM output. Although present-day sea ice is relatively well simulated by the CGCM on a global scale [see *Bush and Philander*, 1999], there is a regional underestimation of sea ice in the North Atlantic. For example, no sea ice is simulated in the marginal ice zone along the Labrador Coast, although this may also be a function of the coarse resolution grid used by the CGCM. We parameterize the sea ice during the LGM by using distributions consistent with the two above listed reconstructions and modify the flux fields accordingly. On the basis of the pattern shown by *Crowley and North* [1991, p. 49, Figure 3.2] for the Northern Hemisphere for January of 18 kyr B.P. (when

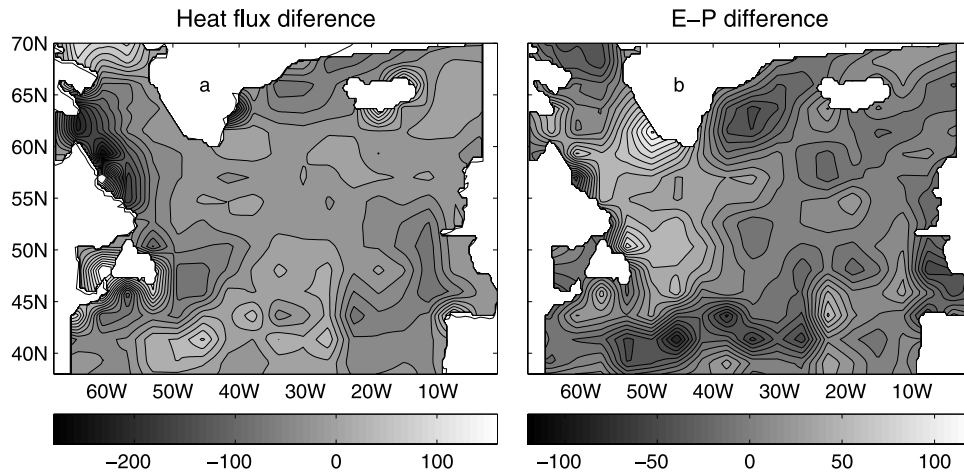


**Figure 1.** Differences in (a) winter (DJF) heat flux ( $\text{W m}^{-2}$ ) and (b) annual E-P ( $\text{cm yr}^{-1}$ ) between the LGM and present, based on CGCM output.

the Labrador Sea was surrounded by the Laurentide, Inuitian, and Greenland ice sheets), we assume sea ice extends southward to  $48^{\circ}\text{N}$  across the entire subpolar region (Figure 2). Here, we assume this “extra” ice is present through the entire winter (December to May) while using the CGCM representation for the rest of the year. A more recent and detailed seasonal reconstruction is the one of *de Vernal and Hillaire-Marcel* [2000], based on sea ice cover during the period from 20 to 16 kyr B.P. We hence assume different seasonality as one moves away from the margins (Figure 2). Perennial sea ice is set for Baffin Bay and along the Labrador shelf. Offshore along the Labrador slope, as well as the Greenland slope, and in Davis Strait, complete ice cover is assumed in winter. For the rest of the Labrador and Irminger Seas, including all areas north of  $55^{\circ}\text{N}$  and west of  $30^{\circ}\text{W}$ , a shorter winter ice season (February through to April) is assumed. Again, except as specified above, the CGCM ice field is then used in all other months. Since the presence of sea ice modifies air-sea fluxes [*Parkinson et al.*, 1987], the paleofluxes are then modified in months when ice cover is present in a given grid cell. Our simple parameterization assumes no freshwater exchange and only limited heat flux exchange (10% of that given by the CGCM [*Parkinson et al.*, 1987]) through the ice, as sea ice is a good insulator.

[10] The same southern boundary condition and restoring buffers in the north as the present are utilized. The reason for this is lack of LGM data. We therefore place our emphasis on the effects of surface atmospheric and sea ice forcing.

[11] We perform four experiments that depend on the surface forcing and sea ice conditions. SOCE is our control experiment with the present-day surface forcing configuration discussed above, and is the same experiment as SOC1 of *Yang* [2005]. This experiment does a good job of reproducing the large-scale circulation of the subpolar North Atlantic, other than the model “Northwest Corner” (near  $51^{\circ}\text{N}$ ,  $43^{\circ}\text{W}$  where the NAC takes a  $90^{\circ}$  turn to the right, defined originally by *Worthington* [1976]) being a bit far to

the east, as shown by *Yang* [2005]. LGME1 is an experiment for the LGM, forced by the LGM surface forcing. LGME2 and LGME3 are experiments for the LGM with modified buoyancy fluxes based upon two sea ice reconstructions. Details on the experiments, including integration lengths, are given in Table 1. The extension of some experiments by 10 years was to confirm that the given simulations were approaching some form of quasi-equilib-

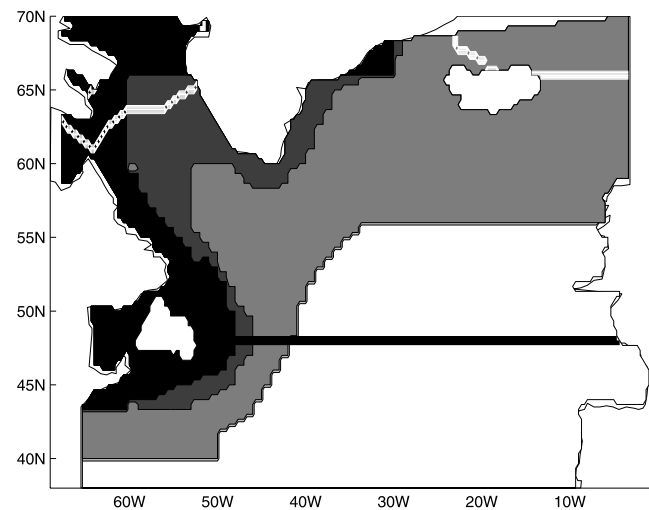


**Figure 2.** LGM sea ice distributions. CGCM output in February (maximum sea ice coverage) is indicated by the thick white line, north of which is covered by sea ice. Sea ice cover north of thick black line ( $48^{\circ}\text{N}$ ) is based on the work by *Crowley and North* [1991]. Shaded sea ice areas are consistent with the work by *de Vernal and Hillaire-Marcel* [2000], with black representing perennial sea ice, dark gray representing winter (December-May) sea ice cover, light gray representing a shorter (February-April) sea ice season, and white area representing ice free.

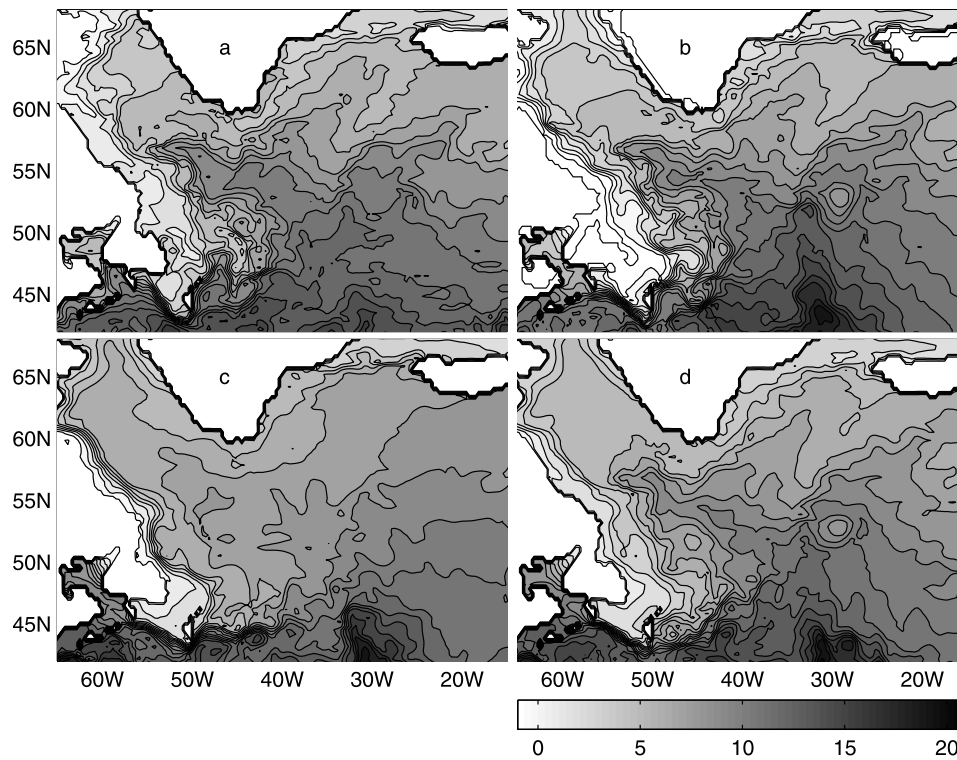


**Figure 3.** Annual temperature at third model level (52 m) for (a) SOCE, (b) LGME1, (c) LGME2, and (d) LGME3.

rium. An extended integration of 80 years for SOCE (discussed by Yang [2005]) further verifies an achievement of the model stability and hence the results obtained by integrations of these lengths (20 or 30 years) are robust.

### 3. Model Results

[12] Wintertime deep convection and LSW formation are observed around  $58.5^{\circ}\text{N}$ ,  $52\text{--}53^{\circ}\text{W}$  in both SOCE and LGME1. The depth of convection reaches 1500 m and 1700 m, respectively. This location, as well as depths ranging from 1500 to 1700 m, have been noted in a number of modern observational studies [e.g., Clarke and Gascard, 1983; Clarke and Coote, 1988; Lilly et al., 1999]. The similarity of LGME1 to SOCE can be attributed to the underrepresentation of sea ice in the Labrador Sea by the CGCM. Without sea ice, strong atmospheric fluxes lead to decrease in buoyancy of the upper waters and enhanced convective overturning. In contrast, there is no LSW formation in either LGME2 or

LGME3. Using proxy data to reconstruct sea surface temperature (SST), sea surface salinity (SSS), surface density, as well as vertical density gradients, [de Vernal and Hillaire-Marcel, 2000; de Vernal et al., 2002] suggest that a strong stratification developed between a shallow, low-salinity surface water layer and the underlying intermediate waters, that was unfavorable for the LSW formation. Although the melt process must be important in terms of providing freshwater to a surface cap, our results support the idea, first suggested by Weaver et al. [2001], that the insulation effect is sufficient on its own to shutdown LSW formation. As the LSW makes up the upper component of NADW, these results support the sensitivity of this water mass (and thus the AMOC) to the sea ice reconstruction and to model flux field. This can be seen by comparing the maximum meridional overturning stream function from each experiment (Table 2).

[13] At present, the NAC is thought to follow the steep topography of the western boundary in a NNE direction

**Table 1.** Summary of Experiments Performed in This Paper

Experiment	Length of Integration, years	Heat Flux	E-P	Wind Stress	Sea Ice
SOCE	30–80	SOC	SOC	ECMWF	no
LGME1	20	CGCM	CGCM	CGCM	white line in Figure 2
LGME2	20	modified CGCM	modified CGCM	CGCM	black line in Figure 2
LGME3	30	modified CGCM	modified CGCM	CGCM	shaded in Figure 2

**Table 2.** Maximum Meridional Stream Function for All Experiments

Experiment	Stream Function, Sv
SOCE	16
LGME1	20
LGME2	6
LGME3	12

from the Southeast Newfoundland Ridge (around 40°N, 45°W) to Flemish Cap (47°N, 45°W), turn northwest into the “Northwest Corner”, then shift sharply toward the northeast around ~50–52°N (discussed by *Luo et al.* [2003]). The NAC is characterized by strong temperature, salinity and hence density gradients as it currently separates warm, saline waters of tropical-subtropical origin and the cold, fresh waters from the Labrador Sea [*Rosby, 1996*]. It thus represents the position of the subpolar front. Figure 3 gives annual temperature fields from the last year of integration (30th year in SOCE, see Table 1 for other experiments) on the third model level (52 m) for all four experiments. The strong temperature and thus density gradients along the NAC path can be clearly seen in all cases. The NACs in SOCE and LGME1 have quite similar flow patterns, flowing northwest into “Northwest Corner” west of 42°W and then turning northeast. The gradients (and thus the flow) are stronger in LGME1 owing to stronger heat loss over the Labrador Sea. An extremely zonal NAC appears several degrees to the south of the ice edge in LGME2. As the Mid-Atlantic Ridge is approached, the flow weakens, leading to only broad and diffuse transport into the eastern basin. The situation in LGME3 is intermediate to LGME1 and LGME2. Initially, the flow is more zonal, similar to LGME2 (albeit with some northward component). However, east of 38°W, the flow begins to resemble LGME1, with a significant meridional component, allowing significant penetration into the Labrador Sea as well as the Iceland Basin. Unlike in LGME1, where the NAC (and thus the (sub)-Arctic Front) is not constrained, in LGME2 and LGME3 the more southerly paths are constrained by the southern limit of sea ice cover.

[14] Atmospheric general circulation model (AGCM) and CGCM experiments indicate a split of the atmospheric wind field into northern and southern branches around the Laurentide Ice Sheet, with the northern branch passing through the Laurentide and Greenland ice sheets and then over the Labrador Sea [*Manabe and Broccoli, 1985; Hall et al., 1996; Bush and Philander, 1999*]. It has been suggested that this modified atmospheric circulation leads to more zonal orientation and a southward shift of the zero line of wind stress curl. This zero line then represents the boundary between subtropical and subpolar gyre and hence the NAC [*Keffer et al., 1988*]. Our results would tend to contradict this hypothesis. In the three LGM experiments, the same paleowind stress pattern is used yet each has a different NAC orientation. Here the NAC path is controlled primarily by the shape and location of the sea ice edge based on the different

reconstructions. That said, since there is no feedback between the winds and the sea ice in our simulations, the NAC has little choice but to follow the ice edge. Analyzing this issue in a fully coupled model will be necessary to support the generality of this conclusion. Still, this result indicates that interaction between ocean circulation and sea ice is very likely to have some measure of control on oceanic meridional heat transport in this region.

#### 4. Discussion and Summary

[15] We examine the impact of atmospheric forcing and its modulation by sea ice in a regional eddy-permitting ocean model of the subpolar North Atlantic. We focus on water mass formation (LSW) and the pathway of the NAC. When using the LGM fluxes from a paleo-CGCM [*Bush and Philander, 1999*], we find a strengthening of LSW formation and the NAC, consistent with the stronger air-sea fluxes believed to have been present during this time. The difference between this result and observations of weakened or curtailed LSW during this time are related to an underestimation of sea ice in the CGCM. When we include extended sea ice, based upon a pair of reconstructions, our results come more into line with that based on the paleoreconstructions. LSW formation is curtailed, leading to a weaker AMOC. The NAC also weakens, and shifts to a more zonal pathway south of the ice edge.

[16] Significantly different circulations, including a wide range of values for the commonly examined AMOC, are found in our simulations with different sea ice reconstructions, one of the less well known paleofields. Our results also support the notion of a positive feedback between ice growth and climate cooling, as suggested by *de Vernal and Hillaire-Marcel* [2000]. In our case, the key aspect of the link is the role of isolating the underlying ocean from the strong atmospheric fluxes, which shuts down intermediate and deep water formation. Our results also present a cautionary tale for the analysis of paleogeneral circulation model results, and therefore emphasize the need for further attempts to accurately refine the LGM sea ice extent, including its seasonal variations (e.g., monthly). This suggests that sea ice reconstructions could and should play a big role in critical appraisal of features of the past used as forcing for climate models.

[17] While the model results capture a key process concerning the impact of surface forcing, one should bear in mind that these simulations cannot be considered as a realistic representation of the LGM response due to the use of present-day data for the boundary data (e.g., northern restoring buffers). Although the NAC path is almost certainly sensitive to the open southern boundary (a limitation of regional ocean models) and thus some of the model details are probably not robust, these factors are not likely to conflict with our first-order conclusions.

[18] **Acknowledgments.** This work is part of the Ph.D. thesis of Duo Yang and was funded by CFCAS (GR-019) and NSERC grants awarded to P.G.M. We would like to thank two anonymous reviewers for their constructive comments that greatly improved the manuscript.

## References

- Adcroft, A., C. Hill, and J. Marshall (1997), Representation of topography by shaved cell in a height coordinate ocean model, *Mon. Weather Rev.*, *125*, 2293–2315.
- Alley, R. B., and P. U. Clark (1999), The deglaciation of the Northern Hemisphere: A global perspective, *Annu. Rev. Earth Planet. Sci.*, *27*, 149–182.
- Boyle, E. A., and L. Keigwin (1987), North Atlantic Thermohaline Circulation during the past 20000 years linked to high-latitude surface temperature, *Nature*, *330*, 35–40.
- Bush, A. B. G., and S. G. H. Philander (1999), The climate of the Last Glacial Maximum: Results from a coupled atmosphere-ocean general circulation model, *J. Geophys. Res.*, *104*, 24,509–24,525.
- Clarke, R. A., and A. R. Coote (1988), The formation of Labrador Sea Water. part III: The evolution of oxygen and nutrient concentration, *J. Phys. Oceanogr.*, *18*, 469–480.
- Clarke, R. A., and J.-C. Gascard (1983), The formation of Labrador Sea Water. part I: Large-scale processes, *J. Phys. Oceanogr.*, *13*, 1764–1778.
- Clarke, R. A., H. W. Hills, R. F. Reiniger, and B. A. Warren (1980), Current system south and east of the Grand Banks of Newfoundland, *J. Phys. Oceanogr.*, *10*, 25–65.
- CLIMAP (1981), Seasonal reconstruction of the Earth's surface at the Last Glacial Maximum, *Geol. Soc. Am. Map Chart Ser.*, MC-36.
- Cottet-Puinel, M., A. J. Weaver, C. Hillaire-Marcel, A. de Vernal, P. U. Clark, and M. Eby (2004), Variation of Labrador Sea Water formation over the Last Glacial cycle in a climate model of intermediate complexity, *Quat. Sci. Rev.*, *23*, 449–465.
- Crowley, T. J., and G. R. North (Eds.) (1991), *Paleoclimatology*, Oxford Univ. Press, New York.
- Curry, R. G., and M. S. McCartney (2001), Ocean gyre circulation changes associated with the North Atlantic Oscillation, *J. Phys. Oceanogr.*, *31*, 3374–3400.
- Curry, R. G., M. S. McCartney, and T. M. Joyce (1998), Oceanic transport of subpolar climate signals to mid-depth subtropical waters, *Nature*, *391*, 575–577.
- Curry, W. B., and G. P. Lohmann (1983), Reduced advection into Atlantic Ocean deep eastern basins during Last Glaciation Maximum, *Nature*, *306*, 577–580.
- de Vernal, A., and C. Hillaire-Marcel (2000), Sea-ice cover, sea-surface salinity and halo-/thermocline structure of the northwest North Atlantic: Modern versus full glacial conditions, *Quat. Sci. Rev.*, *19*, 65–85.
- de Vernal, A., C. Hillaire-Marcel, W. R. Peltier, and A. J. Weaver (2002), Structure of the upper water column in the northwest North Atlantic: Modern versus Last Glacial Maximum conditions, *Paleoceanography*, *17*(4), 1050, doi:10.1029/2001PA000665.
- Dickson, R. R., J. R. N. Lazier, J. Meincke, P. Rhines, and J. Swift (1996), Long-term coordinated changes in the convective activity of the North Atlantic, *Prog. Oceanogr.*, *38*, 241–295.
- Fairbanks, R. G. (1989), A 17,000-year glacio-eustatic sea level record: Influence of glacial melting rates on Younger Dryas event and deep-ocean circulation, *Nature*, *342*, 637–642.
- Grey, S. M., and K. Haines (1999), Climatological hydrography of the North Atlantic, *Int. WOCE Newsl.*, *36*, 23–25.
- Hall, N. M. J., P. J. Valdes, and B. Dong (1996), The maintenance of the last great ice sheets: A UGAMP GCM study, *J. Clim.*, *9*, 1004–1019.
- Josey, S. A., E. C. Kent, and P. K. Taylor (1998), The Southampton Oceanography Centre (SOC) Ocean-atmosphere heat, momentum and freshwater flux atlas, Rep. 6, Southampton Oceanogr. Centre, Southampton, U.K.
- Keffer, T., D. G. Martinson, and B. H. Corliss (1988), The position of the Gulf Stream during Quaternary glaciations, *Science*, *241*, 440–442.
- Lilly, J. M., P. B. Rhines, M. Visbeck, R. Davis, J. R. N. Lazier, F. Schott, and D. Farmer (1999), Observing deep convection in the Labrador Sea during winter 1994/95, *J. Phys. Oceanogr.*, *29*, 2065–2098.
- Lozier, M. S., W. B. Owens, and R. G. Curry (1995), The climatology of the North Atlantic, *Prog. Oceanogr.*, *36*, 1–44.
- Luo, Y., H. Zhang, M. D. Prater, and L. M. Rothstein (2003), Warm water pathways, transports, and transformations in the northwestern North Atlantic and their modification by cold air outbreaks, *J. Geophys. Res.*, *108*(C4), 3129, doi:10.1029/2002JC001442.
- Manabe, S., and A. J. Broccoli (1985), The influence of continental ice sheets on the climate of an ice-age, *J. Geophys. Res.*, *90*, 2167–2190.
- Marchitto, T. M., Jr., D. W. Oppo, and W. B. Curry (2002), Paired benthic foraminiferal Cd/Ca and Zn/Ca evidence for a greatly increased presence of Southern Ocean Water in the glacial North Atlantic, *Paleoceanography*, *17*(3), 1038, doi:10.1029/2000PA000598.
- Miller, J. R., and G. L. Russell (1989), Ocean heat transport during the Last Glacial Maximum, *Paleoceanography*, *4*, 141–155.
- Myers, P. G. (2002), SPOM: A regional model of the sub-polar North Atlantic, *Atmos. Ocean*, *40*, 445–463.
- NOAA (1988), Digital relief of the surface of the Earth, *Tech. Rep. Data Announc. 88-mgg-02*, Natl. Geophys. Data Center, Boulder, Colo.
- Oppo, D. W., and R. G. Fairbanks (1987), Variability in the deep and intermediate water circulation of the Atlantic Ocean during the past 25,000 years: North Hemisphere modulation of the Southern Ocean, *Earth Planet. Sci. Lett.*, *86*, 1–15.
- Parkinson, C. L., J. C. Comiso, H. J. Zwally, D. J. Cavalieri, P. Gloersen, and W. J. Campbell (1987), Arctic Sea Ice, 1973–1976: Satellite passive-microwave observations, *NASA Spec. Publ.*, SP-489.
- Rosati, A., and K. Miyakoda (1988), A general circulation model for upper ocean simulation, *J. Phys. Oceanogr.*, *18*, 1601–1626.
- Rosby, T. (1996), The North Atlantic Current and surrounding waters: At the crossroads, *Rev. Geophys.*, *34*, 463–481.
- Ruddiman, W. F., and A. McIntyre (1977), Late quaternary surface ocean kinematics and climate change in the high-latitude North Atlantic, *J. Geophys. Res.*, *82*, 3877–3887.
- Ruddiman, W. F., and A. McIntyre (1984), Ice-age thermal response and climatic role of the surface North Atlantic Ocean, 43°–63°, *Geol. Soc. Am. Bull.*, *95*, 381–396.
- Rutberg, R. L., S. R. Hemming, and S. L. Goldstein (2000), Reduced North Atlantic Deep Water flux to the glacial Southern Ocean inferred from neodymium isotope ratios, *Nature*, *405*, 935–938.
- Seidov, D., and B. J. Haupt (1997), Simulated ocean circulation and sediment transport in the North Atlantic during the Last Glacial Maximum and today, *Paleoceanography*, *12*, 281–305.
- Seidov, D., and M. Maslin (1996), Seasonally ice free glacial Nordic Seas without deep water ventilation, *Terra Nova*, *8*, 245–254.
- Seidov, D., M. Samthein, K. Statterger, R. Prien, and M. Weinelt (1996), North Atlantic ocean circulation during the Last Glacial Maximum and subsequent meltwater event: A numerical model, *J. Geophys. Res.*, *101*, 16,305–16,332.
- Trenberth, K. E., W. G. Large, and J. G. Olson (1990), The mean annual cycle in global ocean wind stress, *J. Phys. Oceanogr.*, *20*, 1742–1760.
- Veum, T., E. Jansen, M. Arnold, I. Beyer, and J. Duplessy (1992), Water mass exchange between the North Atlantic and the Norwegian Sea during the past 28,000 years, *Nature*, *356*, 783–785.
- Wallace, D. W. R., and J. R. N. Lazier (1988), Anthropogenic chlorofluoromethanes in newly formed Labrador Sea Water, *Nature*, *332*, 61–63.
- Weaver, A. J., M. Eby, A. F. Fanning, and E. C. Wiebe (1998), Simulated influence of carbon dioxide, orbital forcing and ice sheets on the climate of the Last Glacial Maximum, *Nature*, *394*, 847–853.
- Weaver, A. J., et al. (2001), The UVic earth system climate model: Model description, climatology, and applications to past, present and future climates, *Atmos. Ocean*, *39*, 361–428.
- Worthington, L. V. (1976), *On the North Atlantic Circulation*, Johns Hopkins Univ. Press, Baltimore, Md.
- Yang, D. (2005), Impact of anomalous surface forcing on the sub-polar North Atlantic: Water mass formation and circulation, Ph.D. thesis, Univ. of Alberta, Edmonton, Canada.

A. B. G. Bush, P. G. Myers, and D. Yang, Department of Earth and Atmospheric Sciences, University of Alberta, Edmonton, AB, Canada T6G 2E3. (andrew.bush@ualberta.ca; pmyers@ualberta.ca; duo@ualberta.ca)